How to cite: Angew. Chem. Int. Ed. 2024, e202402965
doi.org/10.1002/anie.202402965

Systems Chemistry Hot Paper

A Minimalistic Covalent Bond-Forming Chemical Reaction Cycle that Consumes Adenosine Diphosphate

Tommaso Marchetti, Benjamin M. W. Roberts, Diego Frezzato, and Leonard J. Prins**

Abstract: The development of synthetic active matter requires the ability to design materials capable of harnessing energy from a source to carry out work. Nature achieves this using chemical reaction cycles in which energy released from an exergonic chemical reaction is used to drive biochemical processes. Although many chemically fuelled synthetic reaction cycles that control transient responses, such as self-assembly, have been reported, the generally high complexity of the reported systems hampers a full understanding of how the available chemical energy is actually exploited by these systems. This lack of understanding is a limiting factor in the design of chemically fuelled active matter. Here, we report a minimalistic synthetic responsive reaction cycle in which adenosine diphosphate (ADP) triggers the formation of a catalyst for its own hydrolysis. This establishes an interdependence between the concentrations of the network components resulting in the transient formation of the catalyst. The network is sufficiently simple that all kinetic and thermodynamic parameters governing its behaviour can be characterised, allowing kinetic models to be built that simulate the progress of reactions within the network. While the current network does not enable the ADP-hydrolysis reaction to populate a non-equilibrium composition, these models provide insight into the way the network dissipates energy. Furthermore, essential design principles are revealed for constructing driven systems, in which the network composition *is* driven away from equilibrium through the consumption of chemical energy.

Introduction

Non-equilibrium behaviour is a key feature of life;[1,2] biological systems perform work, exploiting high-energy structures that consume energy to persist.[3] Commonly, biological systems use phosphoanhydride (e.g. adenosine triphosphate (ATP)) hydrolysis as an energy currency within a chemical reaction cycle to drive biochemical processes away from equilibrium.[4] The emergence of such dissipative cycles is not fully understood, though they must have played a crucial role in the origin of life as they are essential in the transition from inactive to active matter.[5–7] The eventual outcome of evolutionary selection on these energy dissipating reaction cycles, is the formation of activated structures that perform non-equilibrium functions, such as movement (e.g. kinesin) or the formation of high-energy structures (e.g. microtubules), driven by catalysing the reaction of high-energy substrates (fuel) to low-energy products (waste).[8]

One way to gain insight in the emergence of driven biochemical reaction networks is the creation of artificial minimal dissipative chemical reaction cycles that control self-assembly using non-biochemical methods, where each step can be studied and understood in chemical detail. To develop such a minimal cycle, there are two basic requirements that must be fulfilled: firstly, the proportion of unassembled and assembled building blocks within the chemical reaction network must change upon the addition of the substrate, adapting to the altered conditions; and secondly, the network must mediate (i.e. catalyse) the substrate to product reaction. This corresponds to 'Class 3' (dissipative) or 'Class 4' (driven) self-assembly,[2] where a network mediates the dissipation of energy via catalysis. In both classes, the presence of two-way feedback between substrate concentration and network composition, allows the system to display preprogrammed and intrinsic adaptive behaviour.

The difference between these two classes is that Class 4 systems possess kinetic asymmetry which enables the system to harness the energy released by the catalytic conversion of fuel to waste to drive the formation of non-equilibrium structures.[2] Despite the ability of Class 3 systems to display transiently altered concentrations of components, potentially giving the impression of a non-equilibrium composition, these effects can only emerge from batchwise operation in which the changing conditions alter the equilibrium concentrations. Under chemostatted conditions, Class 3 systems can never show a non-equilibrium distribution.[2,9,10] It has been rigorously shown that under chemostatted conditions chemical reaction networks cannot be driven away from equilibrium without kinetic asymmetry and cannot transduce energy (e.g. from a chemical reaction) in order to store energy or perform useful work.[9–12] The presence of kinetic asymmetry in reaction networks such as in Figure 1, establishes a so-called information ratchet mechanism,[9–15] in which a stochastic process can be rectified by controlling the

[*] Dr. T. Marchetti, Dr. B. M. W. Roberts, Dr. D. Frezzato, Prof. L. J. Prins
Department of Chemical Sciences
University of Padua
Via Marzolo, 1, 35131 Padua (Italy)
E-mail: diego.frezzato@unipd.it
leonard.prins@unipd.it

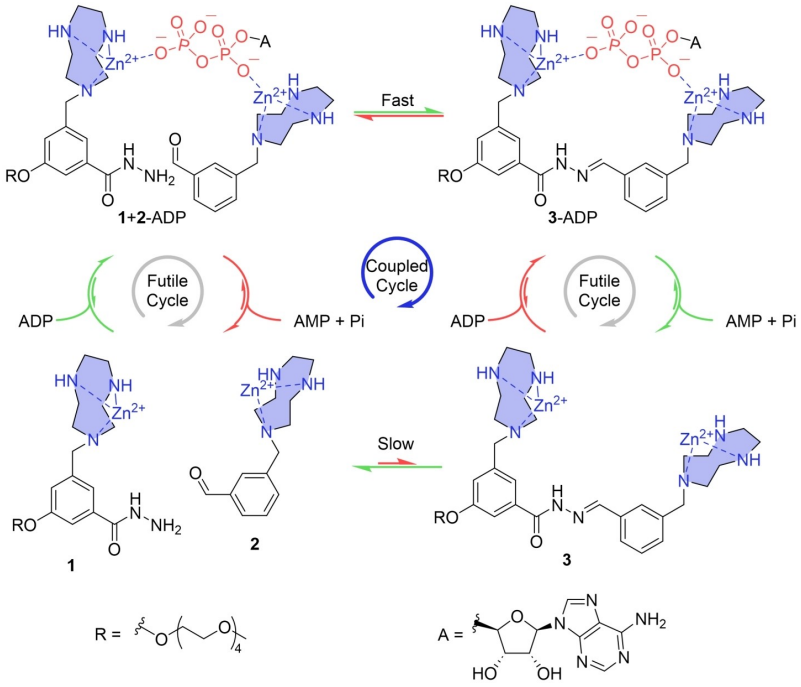

Figure 1. A simplified schematic representation of the key reactions involved in the reaction network. ADP binds to the TACN·Zn(II) head-group (blue) on hydrazide **1** and aldehyde **2** (bottom left to top left, green) which removes electrostatic repulsion between the reactants and templates the formation of hydrazone **3** (top left to top right). ADP hydrolysis is catalysed by TACN·Zn(II) (top right to bottom right, green) and cooperative catalysis makes hydrazone **3** more catalytically active than the reactants. The blue circular arrow and green reaction arrows indicate the forward pathway of the ADP hydrolysis/hydrazone bond formation coupled cycle, red arrows indicate the backward coupled pathway and the grey circular arrows indicate the futile reaction cycles where ADP is hydrolysed with no effect on hydrazone bond formation. The species **1**+**2**-ADP is representative of both species **1** and **2** individually binding ADP and is not used in the full reaction Scheme (see Figure 3 and Supporting Information Section S2).

relative rates at which different species within a network react.[16]

In the last decade, much progress has been made in understanding energy storage and release in (bio)molecular systems and this knowledge has inspired the development of artificial structures with similar properties.[2,13,17–27] However, despite the fact that numerous 'fuelled' systems have now been reported, it has hitherto proven difficult, outside of the context of molecular pumps,[28,29] to understand whether the energy released from the fuel-to-waste reaction is effectively (partially) stored in the system.[30] It can be very difficult to tell whether altered concentrations of network components in response to a stimulus indicate a kinetically controlled non-equilibrium state (Class 4) or a thermodynamically controlled equilibrated adaption (Class 3). This analysis is hampered by the complexity that originates from the numerous kinetic parameters that govern such cycles. Yet, a full understanding of the chemical, functional and organisational principles that define dissipative reaction cycles is essential for comprehending the origin of life and for the development of active synthetic matter.

Here, we show a minimalistic chemical reaction network in which adenosine diphosphate (ADP) induces the formation of a catalyst for its own destruction. The formation of a hydrazone bond between a hydrazide (**1**) and an aldehyde (**2**), each bearing a 1,4,7-triazacyclononane (TACN)·Zn(II) moiety, forms the divalent catalyst (**3**). The hydrazone condensation is accelerated by the addition of ADP which removes electrostatic repulsion between the reagents, stabilising the transition state.[31] ADP binding also stabilises hydrazone **3** with respect to **1** and **2**, biasing the equilibrium towards the product. As well as binding ADP more strongly, hydrazone **3** is a better catalyst for ADP hydrolysis compared to the starting compounds **1** and **2**, resulting in a more rapid formation of adenosine monophosphate (AMP) and phosphate. As these waste products do not stabilise **3** as effectively as ADP, a spontaneous reduction in the concentration of **3** was observed upon ADP depletion. The minimalistic nature of this system enabled the determination of all kinetic parameters within the chemical reaction network, which permits an analysis of the energy transfer between components of the system. The kinetic model indicates that despite the presence of kinetic asymmetry in the system, the non-equilibrium currents remain below the experimental detection limits. However, the full knowledge of all kinetic parameters allowed us to identify the reason for the low efficiency of the system. Rapid (diffusion limited) exchange of ADP and AMP between the bound and unbound state establishes kinetically preferred pathways that decouple ADP hydrolysis and hydrazone bond formation. The result is that, despite involving some of the same intermediates, these two reaction pathways are independent of each other, so that energy released from ADP hydrolysis is not used to drive the hydrazone reaction to a non-

equilibrium composition. Based on this insight, we propose key design principles for the realisation of driven self-assembly systems.[2]

Results and Discussion

Experimental design: We recently described the formation of a hydrazone bond driven by an energy ratchet mechanism between hydrazide **1** and aldehyde **2**, both equipped with a TACN·Zn(II)-complex.[31] The addition of ATP was used to accelerate the reaction and to stabilise the hydrazone bond. ATP hydrolysis was mediated by an enzyme and installed a kinetically stable state in which the concentration of hydrazone **3** was higher than at equilibrium, storing some of the energy released by ATP hydrolysis in a high-energy non-equilibrium state.

Follow up studies of this system revealed that when raised to an elevated temperature (70 °C), hydrazone **3** itself catalysed the hydrolysis of ATP. The observation of spontaneous catalysis by the system, i.e. without an enzyme, is of key importance as it demonstrates that the phosphoanhydride hydrolysis is mediated by the network as a whole, which is essential for developing a dissipative or a driven network.

The formation of **3** was studied at 70 °C (D_2O, pD = 7.4) by ^{1}H NMR, in the presence and absence of ADP (Figure 2), which was used instead of ATP to reduce the complexity of the system, since ADP only contains a single phosphoanhydride bond. A 50-fold acceleration in formation was observed compared to the untemplated reaction and the conversion of **1** + **2** to **3** was more than doubled from 21 % to 44 % (Figure 2a, Supporting Information Section S5.1). The effect of the waste mixture (AMP + Pi) on hydrazone formation was also studied. While the waste both stabilised **3** and accelerated its formation, the magnitude of the effects was smaller than with ADP, showing a 9-fold increase of rate compared with the untemplated reaction and a yield of 34 % (Figure 2a, Supporting Information Sections S4.5). The increased activity of ADP can be explained by its stronger multivalent effect compared to AMP, the larger charge providing greater stabilisation to hydrazone by more effectively removing electrostatic repulsion between head groups.

^{1}H NMR titrations (D_2O, 70 °C, pD = 7.4) showed a binding affinity between ADP and both **1** and **2** in the order of $10^5\ M^{-1}$ (Supporting Information Section S3.1). Direct quantification of the binding strength of **3** with ADP was not possible due to the high affinity, however the 1:1 association constant can be inferred from the relative stabilisation of **3** compared to **1** and **2** in the presence of ADP, owing to thermodynamic consistency rules (Supporting Information Section S3.3). This analysis revealed that the binding constant between ADP and **3** is an order of magnitude higher than the constants measured for **1** and **2**, resulting in an affinity in the order of $10^6\ M^{-1}$. Further titrations showed that the affinity between **1**, **2** and **3** with AMP + Pi mixtures is at least ~2 orders of magnitude lower than for ADP (in the order of $10^3\ M^{-1}$ for compound **1** and **2**

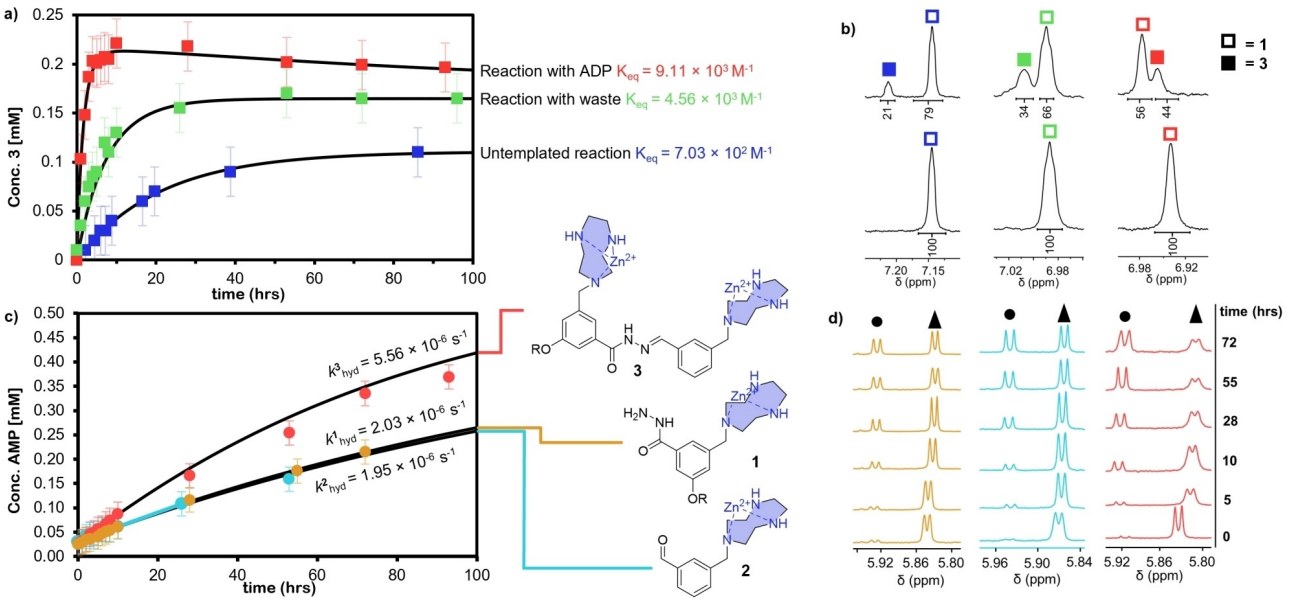

Figure 2. Kinetic experiments for determining the rate of hydrazone formation and ADP hydrolysis a) Graph representing the concentration profile of hydrazone **3** over time after heating an equal mixture of **1** and **2** (0.5 mM) at 70 °C, pD = 7.0 (HEPES buffer, 10 mM) with ADP (red), AMP + Pi (green) and untemplated (blue). b) Partial ^{1}H NMR spectra showing the equilibrated (top) and initial (bottom) signals corresponding to the hydrazide **1** (hollow square) and hydrazone **3** (filled square) of the untemplated reaction (blue), reaction with AMP + Pi (green) and reaction with ADP (red). The different chemical shifts are caused by the ADP or AMP binding. c) Concentration profile of AMP over time after heating ADP (0.5 mM) at 70 °C, pD = 7.0 (HEPES buffer, 10 mM) with **1** (1 mM, orange), **2** (1 mM, turquoise) and **1** + **2** (0.5 mM each, red). d) Partial ^{1}H NMR spectra showing the rate of ADP hydrolysis (triangles) and AMP production (circles) over time. Fittings were obtained by kinetic models (see Supporting Information Section S4 and S5).

and in the order of $10^4\,M^{-1}$ for compound **3** (Supporting Information Sections S3.2, S3.3)).

The phosphoanhydride bond in ADP and ATP is known to be very stable under physiological conditions,[4,32] but it has been reported that phosphoanhydride hydrolysis is catalysed at higher temperatures in the presence of azacrown macrocycles[33,34] or metal cation complexes,[35] similar to the TACN·Zn(II) complexes used here. Since TACN·Zn(II) catalysts are known to exhibit cooperativity when catalysing (P-centred) hydrolysis reactions,[36–38] it was expected that ditopic hydrazone **3**, with two TACN·Zn(II) residues, would function as a better catalyst than either monotopic species **1** or **2**. Catalysis of ADP hydrolysis by TACN·Zn(II)-containing molecules **1**–**3** with a constant head-group concentration of 1 mM was studied by ^{1}H NMR, following the chemical shift of ribose ($\delta_H = 5.90$ to 5.95 ppm, Figure 2d). Even in the presence of a catalyst, ADP hydrolysis is slow, so an elevated temperature (70 °C) was used to achieve ADP hydrolysis on a reasonable timescale. Because the phosphoester bond is much more stable than the phosphoanhydride bond, <5% conversion of AMP into adenosine + Pi was observed after 141 hours which could be safely neglected in kinetic models (Supporting Information Section S5.2). Hydrolysis mediated by **1** and **2** occurs at a similar rate, $k^{\mathbf{1}}_{hyd} = 2.03\times10^{-6}\,s^{-1}$ and $k^{\mathbf{2}}_{hyd} = 1.95\times10^{-6}\,s^{-1}$ (Figure 2c, Supporting Information Sections S4.2 and S4.3). ADP hydrolysis mediated by pure hydrazone **3** at 70 °C was not possible to follow since hydrazone equilibration $\mathbf{1}+\mathbf{2}\rightleftharpoons\mathbf{3}$ occurs on a shorter timescale ($k_{obs}\approx7\times10^{-5}\,s^{-1}$) than ADP hydrolysis. Instead, **1**, **2** and ADP were mixed all at 0.5 mM concentration and the hydrolysis of ADP was followed, to extrapolate the rate constant for catalysis by **3** alone. A 2.8-fold increase in the rate constant for **3**-catalysed ADP hydrolysis was found compared to the reaction catalysed by **1** and **2** with a $k^{\mathbf{3}}_{hyd} = 5.56\times10^{-6}\,s^{-1}$, as determined from a fitted kinetic model (Figure 2c, Supporting Information Section S5.2). These experiments indeed demonstrate an autonomous system where ADP enables the synthesis of a transient catalyst, i.e. hydrazone **3**, that is a more efficient catalyst towards phosphoanhydride hydrolysis compared to the starting building blocks **1** and **2**.

The way in which the reaction system adapts to the ADP concentration and makes itself more suitable for ADP hydrolysis is reminiscent of the responsive behaviour seen in natural metabolic cycles that are the basis for controlling responses to stimuli and performing homeostatic or self-regulating processes.[39] Faster catalysis of ADP hydrolysis by hydrazone **3** functions as 'chemical gating' (i.e. a difference in the rate of a reaction (e.g. ADP hydrolysis) as part of a forward or backward pathway) and can be used to help realise a kinetically asymmetric reaction network and hence an information ratchet mechanism.[9–14]

Kinetic modelling: A transient increase in concentration of **3** was seen upon addition of ADP, however it was unknown whether this was the result of a kinetically controlled driven system (Class 4) with consequent energy storage,[10,30,40] or a thermodynamically controlled adaptation of the system towards a changing ADP concentration, with all species equilibrated according to the concentration of templating anions (Class 3).[2]

Compared with biochemical reaction networks,[4,39] fuelled self-assembly processes and other artificial responsive systems,[17,18,27,19–26] the present reaction system is relatively simple, making it well suited to quantification of reaction parameters. Accordingly, a mass action kinetic model was built describing the chemical reaction network (Figure 3a), based (as far as possible) on independently measured or quantified rate constants (black lines, Figure 2a,c—see Supporting Information Sections S2–S5 for details). Not only does fitting such a model to experimental data test whether the reaction network is understood, but it also provides a tool to perform simulations in which specific parameters can be altered to predict the behaviour of the system under new conditions.[9–14]

The fitted constants indicated the presence of kinetic asymmetry in the network, due to the relative stabilisation of hydrazone **3** by ADP, more rapid hydrolysis of ADP when bound by **3**, as well as the statistical preference for ADP to bind either **1** or **2** (Supporting Information Section S8). However, the model also showed that for the entire duration of the experiment the concentrations of **1**, **2** and **3** remained equilibrated (within error) with respect to the transient ADP concentration (Supporting Information Section S6.5), indicating that the increased hydrazone concentration was a result of thermodynamic stabilisation rather than kinetic selection. That is, despite the presence of kinetic asymmetry in the reaction network, energy consumption does not lead to non-equilibrium concentrations. This suggests that the ADP hydrolysis/hydrazone bond formation coupled cycle (blue circular arrow in Figure 1) is not the primary reaction cycle in control of the chemical processes occurring in the network. Therefore, further analysis of the kinetic model was required to study the interdependence between the driving (ADP hydrolysis) and driven (hydrazone formation) reactions.

Tagged molecule simulations: Despite the minimalistic features, the system still involves a very high level of complexity as a result of the many non-covalent interactions between the reaction components (Figure 3a). To facilitate analysis, we considered the reaction cycle from the point of view of a single 'tagged' molecule which can react and move between different species (sites) within the reaction (sub)network via a stochastic Markov jump process (Figure 3b,c).[41–44] The approach considers only the reactions in which the tagged species can participate, so the 'tagged **1**' and 'tagged **2**' methods provide slightly different viewpoints of the overall reaction network. At steady state, the concentrations of all species are constant, so the jump rate constants for the tagged molecule can be deduced from the fitted rate constants for each reaction and the steady state concentrations of the species within the network. This allows the flux across each reaction jump to be calculated, and in turn the net current. Considering only one molecule significantly simplifies the analysis and makes it possible to inspect the behaviour of reaction networks at the level of individual transitions, whereas traditional methods require the consideration of the network as a whole. This is

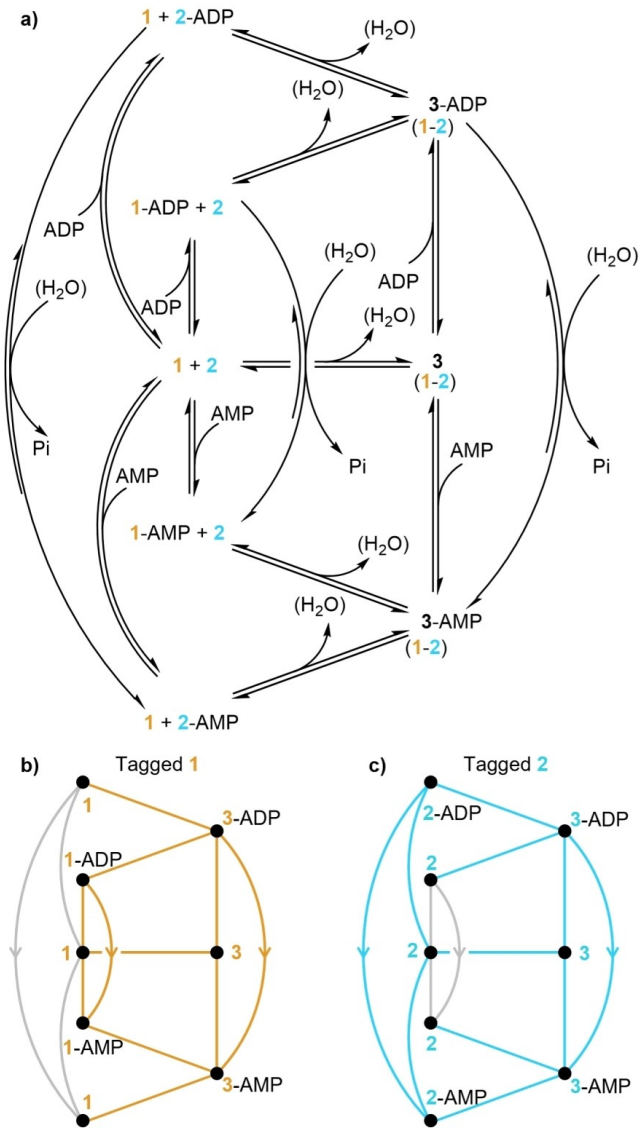

Figure 3. a) The full reaction scheme used for modelling the behaviour of the network with a tagged molecule analysis. Colours show various species within the network to which a 'tag' can be applied. Parentheses are used to indicate that water is treated as implicit in the kinetic model due the high concentration relative to other species.The network can be qualitatively simplified into the reaction cycle shown in Figure 1. b) The network available to tagged **1** and c) the network available to tagged **2** are shown with coloured transitions indicating the jumps in which the tagged molecule participates, while grey transitions are unseen. Different aspects of the network are seen by different tagged molecules, so each provides a different perspective on the network. The arrows indicate the direction of transitions that are especially exergonic (ADP hydrolysis) and so can be considered to proceed almost entirely in the direction depicted. All other transitions experience significant flux in both directions.

especially useful where non-equilibrium behaviour may only be seen in some subnetworks and may not be as apparent across the entire reaction network.[45]

The model was constructed using the kinetic constants obtained from experimental measurements and fitting the mass action kinetic model. We particularly focused on the ideal case of steady state conditions with chemostatted concentrations of ADP, AMP and phosphate (Supporting Information Section S6.4), which ensures that any non-equilibrium concentration must originate from an information ratchet. Following the path of single molecules in this manner highlights the link between the stochastic dynamics at the single molecule level, which enables the exploration of the molecular ratcheting phenomenon from the point of view of a 'molecular reporter', and the deterministic, mass action kinetics commonly used to describe such processes. From the tagged molecule simulations, currents can be extracted which express the average net number of times the tagged molecule undergoes a given reaction within the network (e.g. ADP templated hydrazone bond formation) per unit time. In the absence of dissipation (e.g. at equilibrium), the current is inherently zero as forward and backward processes are balanced.

It was found that, under simulated chemostatted conditions, the net current across the ADP templated hydrazone formation reaction, which reports the current within the forward coupled cycle (Figure 1 green arrows) less that of the backward coupled cycle (Figure 1 red arrows), has to be taken as zero in practice: numerically it was found $<10^{-10}\,s^{-1}$, in the order of the spurious currents in the equilibrated system (Supporting Information Section S6.4). Indeed, the coupled cycles (blue circular arrow, Figure 1) are almost completely suppressed by the presence of uncoupled 'futile cycles' (grey circular arrows, Figure 1) in which ADP hydrolysis is catalysed without altering the state of the hydrazone equilibrium. Hence, the simulations reveal that the experimentally observed transient change in hydrazone concentration is an adaptation to the changing ADP concentration and the building blocks (**1** and **2**) and product (**3**) remain almost equilibrated throughout (Class 3 behaviour). The reason for this is that ADP and AMP exchange in the equilibria (**1**+**2**)+ADP/AMP⇌(**1**+**2**)-ADP/AMP and **3**+ADP/AMP⇌**3**-ADP/AMP are rapid compared to ADP hydrolysis, precluding the development of non-equilibrium concentrations upon energy dissipation. The presence of these rapid transitions establishes 'slip cycles' which involve thermodynamically controlled hydrazone formation without ADP hydrolysis. The presence of these slip cycles tends to reduce the directionality of the network (for a more detailed discussion see Supporting Information Section S8).[9–15,45]

Exploration of other kinetic regimes: To test the hypothesis that the fast (diffusion limited) ADP/AMP association/dissociation is culpable for preventing the system from reaching a non-equilibrium composition through the presence of rapid futile and slip cycles, we used simulations to investigate the effect of slowing down host–guest exchange without altering any of the other parameters of the system, such as the binding constants or the kinetic asymmetry. This is schematically illustrated by the introduction of hypothetical capsules around the Zn(II) binding sites (Figure 4, bottom) which solely generate a kinetic barrier for anion exchange. For each chosen value of the exchange rate, the current was calculated for all reactions from the viewpoint of tagged **1** or **2** (Supporting Information

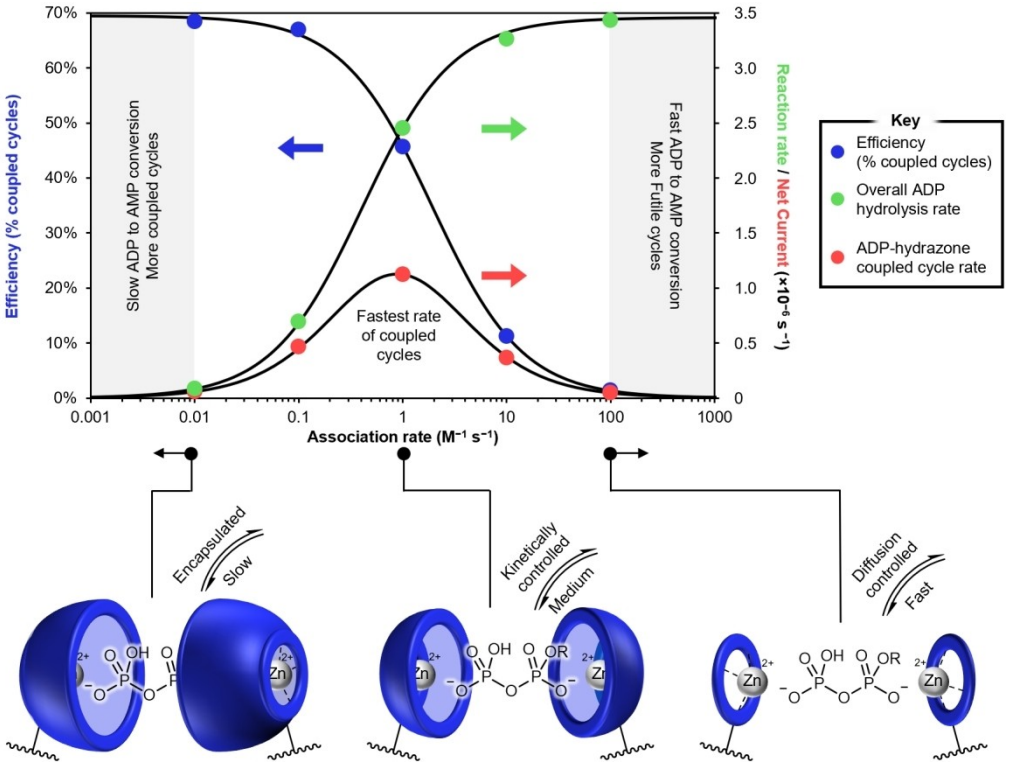

Figure 4. Plot showing the simulated effects at steady state of ADP/AMP exchange rate on the current in the driven ADP templated hydrazone forming reaction, and hence the coupled cycle (red), overall rate of ADP hydrolysis per TACN pair (green) and the efficiency (blue) with unbound ADP, AMP and phosphate chemostatted at 0.005 mM and with the initial concentrations of **1** and **2** at 0.5 mM. The current in the driven reactions is found using tagged molecule simulations following either **1** or **2**, and summing relevant contributions, ADP hydrolysis rate is identified using mass action kinetics and normalised according to the maximum theoretical concentration of **3**, while the efficiency, the ratio between coupled current and ADP hydrolysis rate is found to be the same following either mass action methods or a tagged single molecule approach (see Supporting Information Section S6.5). A trade-off between the efficiency and the overall rate of ADP hydrolysis is required to maximise the rate of the ADP-hydrazone coupled cycle. The exchange rate could potentially be controlled by the formation of full or partial capsule structures which would kinetically control the rate of exchange between bound and solution phase ADP/AMP. Note that the hypothetical blue capsules are for illustrative purposes only, to indicate slower exchange through steric restriction.

Section S6.4). The net current on the coupled cycle (Figure 4, red points) was given by the current across the ADP templated hydrazone formation reactions, since the coupled cycle is the only way of generating a non-zero net flux in this reaction at steady state. The total rate of ADP hydrolysis (Figure 4, green points) was calculated using mass action kinetics and the simulated steady state concentrations of each species, normalised to the maximum theoretical concentration of **3**. The efficiency of the network (Figure 4, blue points) is defined as the proportion of ADP hydrolysis events that contribute to the net forward coupled cycle and so drive the system to a non-equilibrium composition. This is the ratio of the current of the coupled cycle with respect to the overall ADP hydrolysis rate and can be found by considering the ratios of currents in a tagged molecule approach, or from the relative rates of the overall ADP hydrolysis and the net forward coupled cycle.

As the ADP and AMP exchange rates are slowed (moving from right to left on the graph in Figure 4), below a rate constant of ~100 $M^{-1} s^{-1}$ for ADP and AMP binding, the overall rate of ADP hydrolysis begins to decrease. This corresponds with the point at which exchange starts to become the 'rate limiting' step for futile cycles shifting the kinetic preferences from the futile to the coupled cycle. At this rate, species also start to move away from their equilibrium concentrations (Supporting Information Section S6.5). Despite the decreasing overall rate, the rate of the coupled cycle initially increases even as anion exchange is slowed. This is because the coupled pathway is not affected as strongly by decreasing the exchange rates as the futile and slip cycles, so suppression of the coupled cycle no longer occurs. The rate of the coupled cycle reaches a maximum with association rate constants of ~1 $M^{-1} s^{-1}$ after which it also decreases as anion exchange becomes rate limiting for the coupled cycle as well as the futile and slip cycles. However, the coupled cycle allows access to both the faster rate of ADP hydrolysis catalysed by **3** and the faster rate of anion exchange by **1** and **2**, so as the rate slows even further, the coupled cycle becomes kinetically preferred over the futile cycles.[46] Consistently with theory,[40,47] the highest efficiency, peaking at around 70 %, is found to be in the regime in which catalysis is slowest, which occurs at the lowest exchange rates. The high efficiency originates from the suppression of the futile and slip cycles under these

conditions. However, future applications will require a trade-off between highest efficiency and faster rates to be practical.[48]

Conclusion

In conclusion, we have developed a system in which ADP stabilises and accelerates the formation of a hydrazone bond, to produce a species which is more catalytically active towards fuel hydrolysis compared to the starting reactants. This system acts as a chemical reaction network where two orthogonal reactions, ADP hydrolysis and hydrazone bond formation, mutually affect each other.

Our system reproduces a phenomenon that is frequently observed in chemically-fuelled self-assembly processes: namely that the batch-wise addition of the chemical trigger results in the transient formation of a structure. The minimalistic nature of our system permitted a full kinetic analysis which revealed that the observed transient increase in hydrazone concentration originates from an adaptation of the equilibrium reaction to the changing ADP concentrations. An out-of-equilibrium state (i.e. a ratio of building blocks **1** and **2** to product **3** that does not correspond to the equilibrium composition) cannot be experimentally detected inside the network because almost all of the energy is dissipated through uncoupled non-productive futile cycles which do not involve hydrazone bond formation. Importantly, the analysis also showed that the presence of kinetic asymmetry in the coupled cycle is by itself not sufficient to drive the system away from equilibrium. Simulations under steady state conditions indicated that the high ADP/AMP exchange rates compared to the rate of hydrazone hydrolysis is responsible for the suppression of the coupled cycle and the dominance of the futile cycles at steady state.

Despite the absence of efficient energy transduction with the experimentally determined rate constants, the availability of a kinetic model provides a valuable tool to evaluate the importance of key kinetic parameters in the system. Indeed, simulations show that by simply reducing the exchange rate by different orders of magnitude, a current and a non-equilibrium composition emerged in the system. It is of interest to notice, that this is reminiscent of biological systems in which the substrate/product exchange is not governed by diffusion but is kinetically controlled by conformational selection (sometimes referred as chemical or kinetic gating).[3,9,10,13] For example, in microtubules, the archetypal biological example of a dynamic out-of-equilibrium structure, the binding and release of fuel and waste is all but prevented by conformational restriction introduced during polymerisation.[2,49,50] Despite the composition of the reported reaction network being purely governed by thermodynamics, it demonstrates an important element for the future development of autonomous systems based on ratchet mechanisms. To create non-equilibrium systems driven by non-covalently catalysed reactions, in addition to kinetic asymmetry, tight kinetic control over exchange rate must be achieved to suppress futile and slip cycles.[9–14] This poses an interesting challenge in the design of life-like self-assembly systems with catalytic properties.

Supporting Information

The authors have cited additional references within the Supporting Information.[51–56]

Acknowledgements

The authors would like to thank Dr Emanuele Penocchio (Northwestern) for useful discussions and help with the analysis of multicyclic networks and Dr Stefan Borsley (Durham) for useful discussion and feedback on the manuscript. Funding from MUR (2022TSB8P7 and P2022ANCEK) and the University of Padova (P-DiSC #CASABIRD2022-UNIPD) is acknowledged.

Conflict of Interest

The authors declare no conflict of interest.

Data Availability Statement

The data that support the findings of this study are available from the corresponding author upon reasonable request.

Keywords: Non-equilibrium processes · Active matter · Chemical reaction networks · Systems chemistry · Self-assembly

[1] R. Pascal, A. Pross, J. D. Sutherland, *Open Biol.* **2013**, *3*, 130156.
[2] K. Das, L. Gabrielli, L. J. Prins, *Angew. Chem. Int. Ed.* **2021**, *60*, 20120–20143.
[3] S. Borsley, D. A. Leigh, B. M. W. Roberts, *Nat. Chem.* **2022**, *14*, 728–738.
[4] C. T. Walsh, B. P. Tu, Y. Tang, *Chem. Rev.* **2018**, *118*, 1460–1494.
[5] M. Aleksandrova, C. Bonfio, *EMBO Rep.* **2022**, *23*, e55679.
[6] D. Deamer, A. L. Weber, *Cold Spring Harb. Perspect. Biol.* **2010**, *2*, a004929.
[7] K. B. Muchowska, S. J. Varma, J. Moran, *Chem. Rev.* **2020**, *120*, 7708–7744.
[8] R. Merindol, A. Walther, *Chem. Soc. Rev.* **2017**, *46*, 5588–5619.
[9] S. Amano, M. Esposito, E. Kreidt, D. A. Leigh, E. Penocchio, B. M. W. Roberts, *J. Am. Chem. Soc.* **2022**, *144*, 20153–20164.
[10] G. Ragazzon, L. J. Prins, *Nat. Nanotechnol.* **2018**, *13*, 882–889.
[11] R. D. Astumian, *Nat. Commun.* **2019**, *10*, 3837.
[12] R. D. Astumian, *Biophys. J.* **2015**, *108*, 291–303.
[13] T. Sangchai, S. Al Shehimy, E. Penocchio, G. Ragazzon, *Angew. Chem. Int. Ed.* **2023**, *62*, e202309501.
[14] R. D. Astumian, *Angew. Chem. Int. Ed.* **2024**, e202306569.
[15] E. Penocchio, G. Ragazzon, *Small* **2023**, *19*, 2206188.
[16] S. Borsley, J. M. Gallagher, D. A. Leigh, B. M. W. Roberts, *Nat. Chem. Rev.* **2024**, *8*, 8–29.

[17] J. Boekhoven, W. E. Hendriksen, G. J. M. Koper, R. Eelkema, J. H. van Esch, *Science* **2015**, *349*, 1075–1079.
[18] B. A. K. Kriebisch, A. Jussupow, A. M. Bergmann, F. Kohler, H. Dietz, V. R. I. Kaila, J. Boekhoven, *J. Am. Chem. Soc.* **2020**, *142*, 20837–20844.
[19] B. Rieß, R. K. Grötsch, J. Boekhoven, *Chem* **2020**, *6*, 552–578.
[20] N. Singh, G. J. M. Formon, S. De Piccoli, T. M. Hermans, *Adv. Mater.* **2020**, *32*, 1906834.
[21] N. Singh, B. Lainer, G. J. M. Formon, S. De Piccoli, T. M. Hermans, *J. Am. Chem. Soc.* **2020**, *142*, 4083–4087.
[22] P. Solís Muñana, G. Ragazzon, J. Dupont, C. Z.-J. Ren, L. J. Prins, J. L.-Y. Chen, *Angew. Chem. Int. Ed.* **2018**, *57*, 16469–16474.
[23] K. Das, H. Kar, R. Chen, I. Fortunati, C. Ferrante, P. Scrimin, L. Gabrielli, L. J. Prins, *J. Am. Chem. Soc.* **2023**, *145*, 898–904.
[24] S. P. Afrose, C. Ghosh, D. Das, *Chem. Sci.* **2021**, *12*, 14674–14685.
[25] S. Bal, K. Das, S. Ahmed, D. Das, *Angew. Chem. Int. Ed.* **2019**, *58*, 244–247.
[26] L. S. Kariyawasam, C. S. Hartley, *J. Am. Chem. Soc.* **2017**, *139*, 11949–11955.
[27] S. Debnath, S. Roy, R. V. Ulijn, *J. Am. Chem. Soc.* **2013**, *135*, 16789–16792.
[28] L. Binks, S. Borsley, T. R. Gingrich, D. A. Leigh, E. Penocchio, B. M. W. Roberts, *Chem* **2023**, *9*, 2902–2917.
[29] L. Feng, Y. Qiu, Q.-H. Guo, Z. Chen, J. S. W. Seale, K. He, H. Wu, Y. Feng, O. K. Farha, R. D. Astumian, J. F. Stoddart, *Science* **2021**, *374*, 1215–1221.
[30] E. Olivieri, J. M. Gallagher, A. Betts, T. W. Mrad, D. A. Leigh, *Nat. Synth.* **2024**, DOI 10.1038/s44160-024-00493-w.
[31] T. Marchetti, D. Frezzato, L. Gabrielli, L. J. Prins, *Angew. Chem. Int. Ed.* **2023**, *62*, e202307530.
[32] J. Rosing, E. C. Slater, *Biochim. Biophys. Acta Bioenerg.* **1972**, *267*, 275–290.
[33] M. W. Hosseini, J.-M. Lehn, K. C. Jones, K. E. Plute, K. B. Mertes, M. P. Mertes, *J. Am. Chem. Soc.* **1989**, *111*, 6330–6335.
[34] M. W. Hosseini, J.-M. Lehn, L. Maggiora, K. B. Mertes, M. P. Mertes, *J. Am. Chem. Soc.* **1987**, *109*, 537–544.
[35] C. Bazzicalupi, A. Bencini, A. Bianchi, A. Danesi, C. Giorgi, C. Lodeiro, F. Pina, S. Santarelli, B. Valtancoli, *Chem. Commun.* **2005**, 2630–2632.
[36] F. Manea, F. B. Houillon, L. Pasquato, P. Scrimin, *Angew. Chem. Int. Ed.* **2004**, *43*, 6165–6169.
[37] L. Prins, F. Mancin, P. Scrimin, *Curr. Org. Chem.* **2009**, *13*, 1050–1064.
[38] A. Pecina, D. Rosa-Gastaldo, L. Riccardi, S. Franco-Ulloa, E. Milan, P. Scrimin, F. Mancin, M. De Vivo, *ACS Catal.* **2021**, *11*, 8736–8748.
[39] M. Reed, J. Best, M. Golubitsky, I. Stewart, H. F. Nijhout, *Bull. Math. Biol.* **2017**, *79*, 2534–2557.
[40] E. Penocchio, R. Rao, M. Esposito, *Nat. Commun.* **2019**, *10*, 3865.
[41] A. Sabatino, D. Frezzato, *J. Chem. Phys.* **2019**, *150*, 134104.
[42] D. Frezzato, *Math. Biosci.* **2021**, *332*, 108518.
[43] A. Sabatino, E. Penocchio, G. Ragazzon, A. Credi, D. Frezzato, *Angew. Chem. Int. Ed.* **2019**, *58*, 14341–14348.
[44] D. Asnicar, E. Penocchio, D. Frezzato, *J. Chem. Phys.* **2022**, *156*, 184116.
[45] E. Penocchio, A. Bachir, A. Credi, R. D. Astumian, G. Ragazzon, *ChemRxiv preprint* **2024**, DOI: 10.26434/chemrxiv-2024-pzhcs.
[46] J. M. Gallagher, B. M. W. Roberts, S. Borsley, D. A. Leigh, *Chem* **2024**, *10*, 855–866.
[47] S. Amano, M. Esposito, E. Kreidt, D. A. Leigh, E. Penocchio, B. M. W. Roberts, *Nat. Chem.* **2022**, *14*, 530–537.
[48] U. Seifert, *Rep. Prog. Phys.* **2012**, *75*, 126001.
[49] G. Margolin, I. V. Gregoretti, T. M. Cickovski, C. Li, W. Shi, M. S. Alber, H. V. Goodson, *Mol. Biol. Cell* **2012**, *23*, 642–656.
[50] D. Seetapun, B. T. Castle, A. J. McIntyre, P. T. Tran, D. J. Odde, *Curr. Biol.* **2012**, *22*, 1681–1687.
[51] T.-L. Hwang, A. J. Shaka, *J. Magn. Reson. Ser. A* **1995**, *112*, 275–279.
[52] S. Hoops, S. Sahle, R. Gauges, C. Lee, J. Pahle, N. Simus, M. Singhal, L. Xu, P. Mendes, U. Kummer, *Bioinformatics* **2006**, *22*, 3067–3074.
[53] L. Onsager, *Phys. Rev.* **1931**, 405–426.
[54] R. Wegscheider, *Zeitschrift für Phys. Chem.* **1901**, *39*, 257–303.
[55] P. N. Brown, G. D. Byrne, A. C. Hindmarsh, *SIAM J. Sci. Stat. Comput.* **1989**, *10*, 1038–1051. The double-precision Fortran subroutine 'DVODE' is available at ODEPACK: Software | Computing (llnl.gov) (last viewed on 29 December 2023).
[56] *GAMS: Module RG in EISPACK.* https://gams.nist.gov/cgi-bin/serve.cgi/Module/EISPACK/RG/7908 (accessed 2024–01-20).

Manuscript received: February 9, 2024
Accepted manuscript online: March 27, 2024
Version of record online: ■■, ■■

Research Articles

Systems Chemistry

T. Marchetti, B. M. W. Roberts, D. Frezzato,* L. J. Prins* — **e202402965**

A Minimalistic Covalent Bond-Forming Chemical Reaction Cycle that Consumes Adenosine Diphosphate

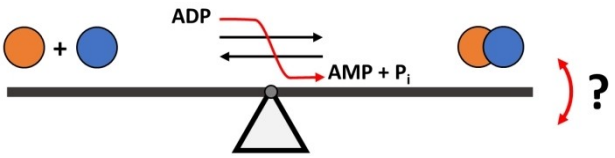

Materials that consume chemical energy are fundamental to the development of synthetic active matter, yet the complexity of their reaction cycles hinders understanding how energy is used. The creation of a fully characterised minimalistic metabolic cycle based on the adenosine diphosphate (ADP) driven assembly of building blocks has allowed insight to be gained into the way energy is dissipated by the network and uncover general design principles for driven systems.